analytical chemistry

pubs.acs.org/ac Article

Use of Cyclic Ion Mobility Spectrometry (cIM)-Mass Spectrometry to Study the Intramolecular Transacylation of Diclofenac Acyl Glucuronide

David Higton,* Martin E. Palmer, Johannes P. C. Vissers, Lauren G. Mullin, Robert S. Plumb, and Ian D. Wilson*

Cite This: *Anal. Chem.* 2021, 93, 7413–7421 Read Online

ACCESS | Metrics & More | Article Recommendations | Supporting Information

ABSTRACT: 1-*β*-*O*-Acyl-glucuronides (AGs) are common metabolites of carboxylic acid-containing xenobiotics, including, *e.g.*, many nonsteroidal anti-inflammatory drugs (NSAIDs). They are of concern to regulatory authorities because of the association of these metabolites with the hepatotoxicity that has resulted in drug withdrawal. One factor in assessing the potential risk posed by AGs is the rate of transacylation of the biosynthetic 1-*β*-*O*-acyl form to the 2-, 3-, and 4-*O*-acyl isomers. While transacylation can be measured using ^{1}H NMR spectroscopy or liquid chromatography-mass spectrometry (LC-MS), the process can be time consuming and involve significant method development. The separation of these positional isomers by ion mobility spectrometry (IMS) has the potential to allow their rapid analysis, but conventional instruments lacked the resolving power to do this. Prediction of the collision cross section (CCS) using a machine learning model suggested that greater IMS resolution might be of use in this area. Cyclic IMS was evaluated for separating mixtures of isomeric AGs of diclofenac and was compared with a conventional ultraperformance liquid chromatography (UPLC)-MS method as a means for studying transacylation kinetics. The resolution of isomeric AGs was not seen using a conventional traveling wave IMS device; however, separation was seen after several passes around a cyclic IMS. The cyclic IMS enabled the degradation of the 1-*β*-*O*-acyl-isomer to be analyzed much more rapidly than by LC-MS. The ability of cyclic IMS to monitor the rate of AG transacylation at different pH values, without the need for a prior chromatographic separation, should allow high-throughput, real-time, monitoring of these types of reactions.

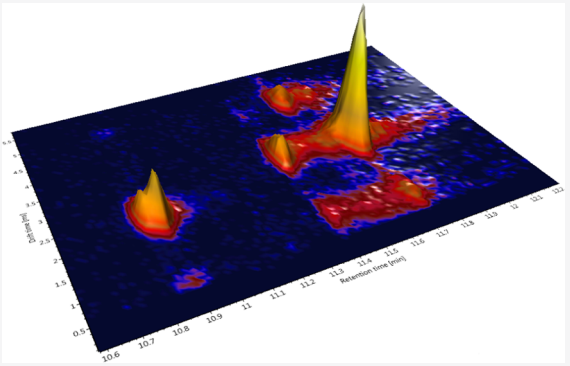

A continuing problem for pharmaceutical discovery and development is the production of reactive and therefore potentially toxic metabolites during the course of the metabolism of new drug candidates. In general, the conjugation of drugs or their metabolites to glucuronic acid produces pharmacologically inactive glucuronides and is correctly seen as a detoxication process. However, in the case of acyl or ester, glucuronidation, an association between their production and drug toxicity, which has led in some instances to drug withdrawal, has been noted. In particular, this has been linked to the toxicity sometimes seen with nonsteroidal anti-inflammatory drugs (NSAIDs), many of which form acyl glucuronides (AGs) and a number of them have been withdrawn from the market due to adverse drug reactions (ADRs).[1−5] Such ADRs have led to regulatory authorities, such as the U.S. Federal Drug Administration, requiring efforts to be made in the toxicological assessment of these AGs. As a result, methods for determining their reactivity have been of increased interest to both medicinal chemists and toxicologists.[6] One property that has been used for assessing the reactivity of acyl glucuronides, and therefore the potential risk posed by them, is the rate of transacylation in aqueous buffer of the biosynthetic 1-*β*-*O*-acyl-AG form to the 2-, 3-, and 4-*O*-acyl isomers. This degradation rate is used as a surrogate for reactivity with proteins.[1−5] Currently, the techniques most frequently used to determine transacylation rates for AGs are ^{1}H NMR spectroscopy, *e.g.*, ref 7, or high-performance liquid chromatography (HPLC) using either UV or MS detection (*e.g.*, refs 8 and 9). However, analysis by either ^{1}H NMR spectroscopy or chromatographic methods is often time consuming. In addition, the development of the separation methods for the isomeric glucuronides may also require optimization for each analyte, making generic "high-throughput" assays for screening or kinetic measurements impractical. As AGs are isomers, an alternative technique to

Received: October 23, 2020
Accepted: April 12, 2021
Published: May 13, 2021

https://doi.org/10.1021/acs.analchem.0c04487
Anal. Chem. 2021, 93, 7413−7421

mass resolution such as ion mobility is needed to resolve the different isomers. The cyclic IMS (cIM)[10] allows ions to pass around the ion mobility device multiple times, thereby providing significantly longer path lengths and hence increased resolution compared to linear IM instruments. Here, the resolution of molecules of similar structures using cIM has been applied to the rapid separation of the 1-β-*O*-acyl glucuronide of the drug diclofenac from its 2-, 3-, and 4-*O*-acyl isomers and to the determination of properties such as their collision cross section and pH-dependent rates of formation.

EXPERIMENTAL SECTION

Chemicals and Reagents. Acetonitrile (Honeywell Research Chemicals) was obtained from Fisher Scientific U.K. (Rugby U.K.), and water was either HPLC grade from the same supplier or from an Elga Ultra Mk2 Water Purification system (High Wycombe, U.K.). Ammonium acetate solution (1 M, pH 5), formic acid, Major Mix IMS/Tof calibration, and sodium formate calibration solutions were obtained from Waters Corporation (Milford, MA). Ammonium acetate was provided by Sigma-Aldrich (Gillingham, U.K.) from which a fresh 1 M ammonium acetate stock was created. Ammonium hydroxide solution obtained from Sigma-Aldrich was used to adjust the pH of the ammonium acetate. The pH values were confirmed by measurement using a Mettler Toledo (Switzerland) Seveneasy pH meter. Diclofenac β-1-*O*-acyl glucuronide (DAG) was synthesized using the published methodology[11] and was greater than 98% pure as assessed by ^{1}H NMR spectroscopy.

Sample Preparation. DAG was dissolved in acetonitrile/water (1:1 v/v) to obtain a 10 mM stock solution. This DAG solution was diluted to 10 μM using 10 mM ammonium acetate solution either diluted with HPLC water at pH 5 (A) or pH 7.8 (B) or from solid using Elga water at pH 8.5 (C). A DAG solution at a concentration of 10 μM in 10 mM ammonium acetate at pH 5 (solution A), to prevent transacylation, was used for the initial method development of the LC-MS method for the separation of the acyl glucuronide mixtures and the multipass ion mobility experiments. Initially, the DAG solution prepared at pH 7.8 (solution B) was left for 22 h at room temperature to allow transacylation to occur and was then used for the initial method of the LC separation and IM methods for the transacylated species. For further method development and kinetic studies, a 10 μM solution of the DAG in 10 mM ammonium acetate buffer at pH 8.5 (solution C) was used. These pH conditions, rather than the more physiological pH of 7.4 normally used (*e.g.*, refs 7, 9), were employed to achieve rapid transacylation.

LC-IM-MS Analyses. LC-IM-MS analyses were performed using an ACQUITY UPLC I-Class FTN (Waters Corporation) coupled to a SYNAPT XS, a Q-IMS-Tof (Waters Corporation). Prior to use, the system was mass-calibrated using sodium formate. Additionally, the Major Mix IMS/Tof calibration solution was used to calibrate the traveling wave ion mobility (TWIMS) device and facilitate the measurement of $^{TW}CCS_{N2}$ values. An ACQUITY UPLC HSS T3, 2.1 mm × 100 mm 1.8 μm column at a temperature of 45 °C was used. Mobile phase A was water with 0.1% formic acid (v/v), and mobile phase B was acetonitrile with 0.1% formic acid (v/v). Separations (0.6 mL/min) were performed using a linear gradient elution program: 0−0.5 min isocratic at 95:5 (A/B); 0.5−15.5 min (50:50), 15.5−16 min (5:95) hold till 18 min and then 18.0−18.1 min (95:5), giving a total analysis time of *ca.* 20 min allowing for column re-equilibration.

The instrument was equipped with an electrospray ion source with the capillary voltage set to 2 kV in a positive ion mode. The desolvation gas flow was 1000 L/h, the desolvation gas temperature was 550 °C, and the source temperature was 120 °C. Data were acquired from m/z 50 to 1200 with a 0.1 s scan time. The linear TWIMS device used nitrogen as the drift gas and had a gas pressure of 3.0 mbar, a traveling wave height of 40 V, and the velocity was set to 650 m/s.

For these, and the infusion experiments described below, the instrument was controlled using MassLynx 4.2. The obtained data were processed using UNIFI 1.9.4 and MassLynx 4.2.

LC-cIM-MS Analyses. Prior to use, the Major Mix IMS/Tof calibration solution (Waters Corporation) was used to calibrate the ion mobility device in a single-pass mode to provide $^{TW}CCS_{N2}$ values, and sodium formate was used to calibrate the time-of-flight analyzer of the mass spectrometer. Incubations were analyzed on an ACQUITY UPLC I-Class Plus system with a tunable UV detector (Waters Corporation) coupled to a SELECT SERIES Cyclic IMS (Waters Corporation), a Q-Tof mass spectrometer equipped with a novel cIM device. The LC column, mobile phase, and gradient conditions were the same as for the LC-IM-MS analysis described previously. The UV detector was set to acquire data at 254 nm.

The instrument was equipped with an electrospray ion source with the capillary voltage set to 2 kV in the positive ion mode and 1 kV in the negative ion mode. The desolvation gas flow was 1000 L/h, the desolvation gas temperature was 550 °C, and the source temperature was 120 °C. MS data were acquired in the positive ion mode using a single pass of the cIM device to obtain CCS values. CCS are a fundamental property of an ion and do not change with multiple passes of the cIM. If the components had not been resolved chromatographically, the measurement of CCS after multiple passes of the cIM would have been beneficial as separation of these components might have been possible with the additional ion mobility resolution. However, as the major components were resolved by LC, the CCS data were acquired using a single pass, allowing comparison with the data acquired in the same manner on the linear IM instrument. The same MS data were gathered again after 8 passes to allow comparison with the infusion data. MS/MS data were acquired in positive and negative modes with trap collision energies of 20 and 15 V, respectively. For all modes, data were acquired from m/z 50 to 1200 with a 0.2 s scan time. The cIM device had a gas pressure of 1.6 mbar, a traveling wave height of 15 V, and the velocity was set to 375 m/s. These settings were also used for the infusion experiments. The data were acquired in a V-mode geometry with a mass resolution of >60 000 FWHM.

For these and infusion experiments, the instrument was controlled using MassLynx 4.2 software. The obtained data were processed using UNIFI 1.9.4, MassLynx 4.2, and DriftScope 2.9. The latter was used to export drift time retained data for further processing using MassLynx 4.2, where arrival time distributions (ATDs) were produced for ions of interest.

Infusion cIM-MS. The incubation solutions were placed on the instrument fluidics, and incubation occurred *in situ* at ambient temperature with the infusion at 5 μL/min into the electrospray ion source of the SELECT SERIES Cyclic IMS. The instrument was operated in the positive ion mode using a capillary voltage of 2 kV and a nitrogen desolvation gas flow of 600 L/h. The desolvation and source temperatures were 280 and 100 °C, respectively. Following separation in the cIM, mass spectra for the various isomers were acquired from m/z 50 to 1200 with a 1 s scan time for 30 s. The separation times for the

https://doi.org/10.1021/acs.analchem.0c04487
Anal. Chem. 2021, 93, 7413−7421

Table 1. t_R Time, $[M + H]^+$ Ion, and Observed and Predicted CCS Values for DAG and Isomers

isomer	t_R (min)[a]	observed m/z (Da)	mass error (ppm)	observed $^{TW}CCS_{N2}$ (Å^2)[a]	observed $^{TW}CCS_{N2}$ difference (%)	predicted $^{TW}CCS_{N2}$ (Å^2)	predicted $^{TW}CCS_{N2}$ difference from observed (%)[a]
1-*O*-acyl	11.61/11.48	472.0560	−0.2	205.3 ± 0.1/203.9 ± 0.1	0.7	202.2	1.5/0.8
2-*O*-acyl	11.73/11.57	472.0559	−0.3	201.1 ± 0.0/201.2 ± 0.2	0.0	199.2	1.0/1.0
3-*O*-acyl	11.43/11.30	472.0562	0.3	200.9 ± 0.1/200.9 ± 0.2	0.0	199.2	0.9/0.9
4-*O*-acyl	10.84− 10.93/10.73	472.0560	−0.1	199.7 ± 0.1/198.8 ± 0.2	0.5	194.7	2.5/2.0

[a]Cyclic IMS/SYNAPT XS. The observed CCS values are the mean of duplicate measurements. Comparing across all four measurements, the intravariability was less than 0.4% for all isomers, which is comparable to other published studies.[21−23]

cIM device were varied to acquire data from 1 to 8 passes of the cIM. In a second experiment, the components with the slowest and fastest migration times were ejected from the device and discarded, and the remaining components underwent a further 8 passes to give a total of 16 passes.[10] For the incubation to determine the kinetics of transacylation at pH 8.5, data were acquired at 0.083, 0.25, 0.5, 1, 1.5, 2, 2.5, 3, 3.5, 4, and 5 h. As indicated, these conditions, rather than the more physiological pH 7.4 often employed (*e.g.*, refs 7, 9), were used to obtain a more rapid rate of transacylation.

CCS Prediction. The gradient boosting (GB) algorithm was used to create a bespoke predictive machine learning-based model using known, experimentally validated $^{TW}CCS_{N2}$ values with relevant molecular descriptors. In the current application, briefly, this was achieved through the use of the XGBoost[12] and RDKit[13] libraries. A nested cross-validation strategy was used that included folds for hyperparameter optimization, using autoML, inside folds for training and testing the model, for which the scikit-learn library[14] was applied, which performs Monte Carlo sampling over the hyperparameters. A more detailed description of the principles, background information, validation, and some basic performance metrics are provided elsewhere.[15,16] Machine learning-based prediction of CCS has been compared (*e.g.*, refs 17, 18) to the computational modeling approach, which predicts and optimizes the 3D structure that is used for theoretical calculation of the CCS. These comparisons show suitability of the machine learning approach for CCS prediction compared to that of computational modeling.

RESULTS AND DISCUSSION

LC, with either UV,[8] MS/MS,[9] or ^{1}H NMR spectroscopy[19] methodology, has previously been extensively used to study the transacylation of acyl glucuronides. One of the main drawbacks of using this type of methodology is that the time taken to separate the various isomers using LC can make it difficult to study the isomerization in real time. This is particularly the case for those acyl glucuronides that rapidly transacylate at physiological pH (especially when incubated in plasma[20]). However, prediction of the CCS values for the biosynthetic 1-*O*-acyl and transacylated 2-, 3-, and 4-*O*-acylated forms of DAG (Table 1) using machine learning suggested that in fact there were indeed likely to be small differences that might be exploited using IMS as a separation technique prior to MS detection. If so, this might enable the rapid determination of transacylation kinetics without the need for chromatography.

LC-IM-MS. To evaluate the use of an IMS-based separation for determining DAG transacylation kinetics, we therefore undertook LC-IM-MS analyses using a SYNAPT XS Q-IMS-Tof mass spectrometer. The purpose of this was twofold. The first was to establish using the current methodology the elution order of the various DAG isomers *via* an optimized UPLC separation to determine the kinetics of transacylation. The second was to determine the CCS for each of the isomeric glucuronides experimentally and compare them with the predicted values. Here, DAG was incubated in 10 mM aqueous ammonium acetate at pH 8.5, at room temperature, for 2 h, and studied using a separation method developed to provide good retention of the 1-*O*-acyl form of DAG, which eluted with a retention time (t_R) of 11.48 min (overall analysis time: 20 min) (Table 1). Based upon comparison with the standard, the disappearance of the 1-*O* DAG, and the sequential appearance of the other forms, the elution order 4 α/β > 3 > 1 > 2-*O*-DAG was established with the latter having a t_R of 11.57 min (Table 1). Clearly, with further optimization, the cycle time could possibly be reduced to *ca.* 15 min to increase throughput and, as the transacylation reaction can be halted by reducing the pH to, *e.g.*, 5, serial samples could be taken at short intervals for subsequent analysis. However, adoption of such a strategy would still limit analysis to *ca.* 4 samples/h. From the data obtained here, the initial half-life (measured up to 1.5 h) of the 1-*O*-acyl DAG was found to be 0.95 h (Figure S1). As can be seen from Figure 1 (which shows the same separation obtained using the LC-UV-CIM-MS), the LC peak shapes of the transacylated isomers are broader than might be expected.

The broadness of these peaks is probably a result of the presence of both α- and β-anomeric forms of the respective AGs (*e.g.*, see ref 7 and references quoted therein). This anomerization is rapid on the LC time scale with interconversion continuing during the separation itself so that even when partially separated, as in the case of 4-*O*-acyl form, the peaks cannot be fully resolved.

When the measured CCS values obtained experimentally were compared with those predicted for the various DAG isomers, the rank order of the isomers based on CCS was consistent between measured and predicted and was in the order 1-*O*-acyl > 2-*O*-acyl > 3-*O*-acyl > 4-*O*-acyl. Thus, it is clear in this case that, despite the differences seen between the calculated and measured CCS values, the predictive machine learning-based model was able to provide guidance with respect to likely differences between similar, but different, isomeric structures. Subsequently, these CCS values were also calculated using a molecular orbital-based approach (MOBCAL)[24] and gave similar results (Figure S2).

However, given the small differences between most of the transacylated forms of DAG, it would not have been possible to measure them separately on the linear TWIMS without prior resolution by LC (Figure S3).

LC-UV-cIM-MS. Again, DAG was incubated at pH 8.5 in 10 mM aqueous ammonium acetate, at room temperature, for 2 h, and samples of these incubations were studied by LC-UV-cIM-MS with 8 passes of the cIM device and using the same LC method as described above. The MS and UV chromatograms are

https://doi.org/10.1021/acs.analchem.0c04487
Anal. Chem. 2021, 93, 7413−7421

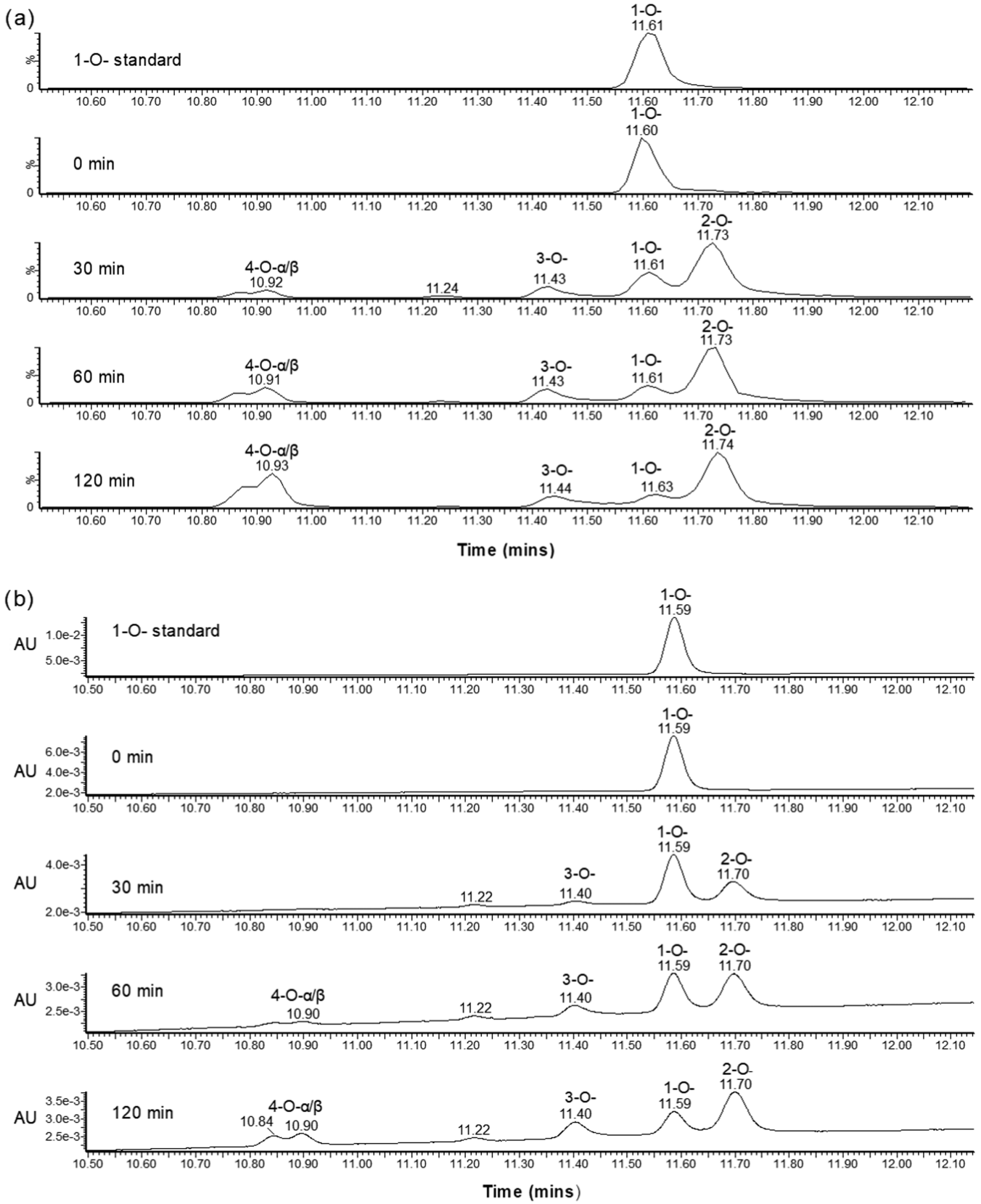

Figure 1. (a) Extracted ion and (b) UV chromatograms for LC-UV-cIM-MS analysis of DAG standard and following incubation for 0, 30, 60, and 120 min at pH 8.5 and room temperature and with 8 passes of the cIM device.

illustrated in Figure 1, and the relative MS and UV responses were similar. The retention times were slightly longer than those observed on the SYNAPT XS due to the extra system volume arising from the presence of the UV detector. Mass spectra of the four isomers obtained in positive ion mode are shown in Figure S4, and product ion mass spectra in positive ion (Figure 2) and

https://doi.org/10.1021/acs.analchem.0c04487
Anal. Chem. 2021, 93, 7413−7421

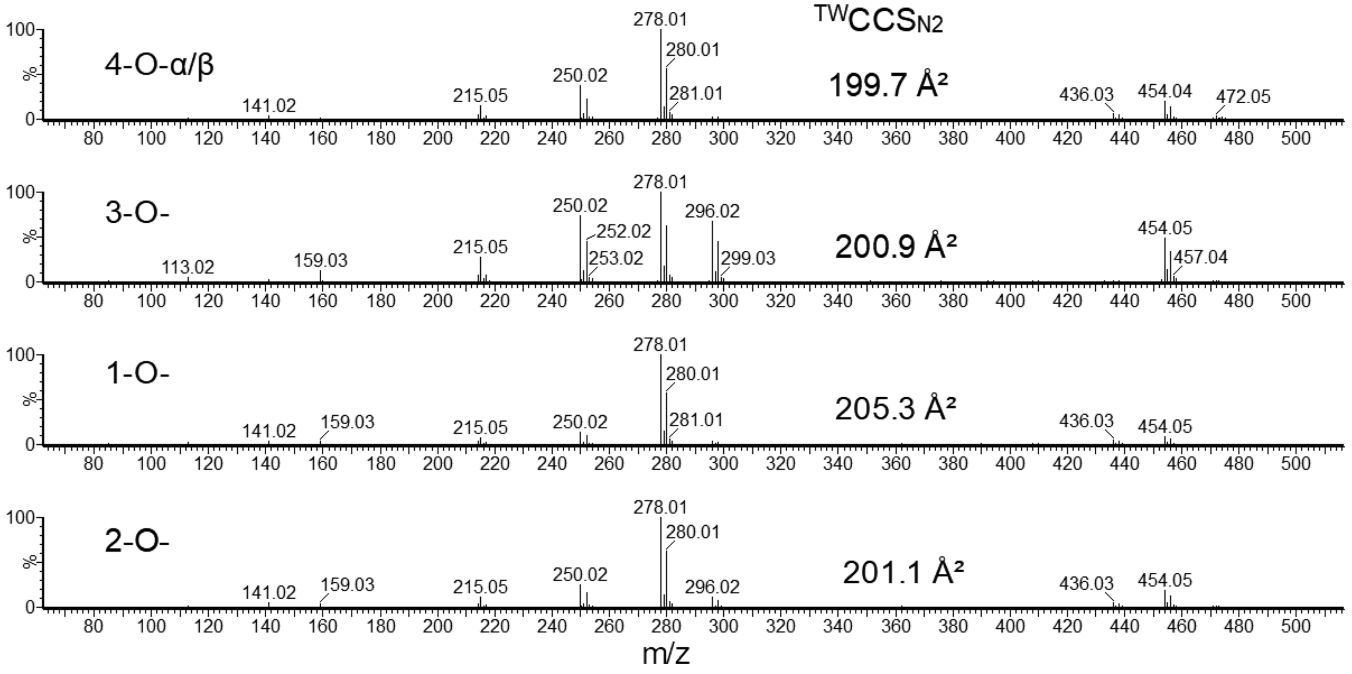

Figure 2. Product ion mass spectra of $[M + H]^+$ (m/z 472) and $^{TW}CCS_{N2}$ for 4-O, 3-O, 1-O, and 2-O isomers obtained from LC-MS/MS analyses of incubation of 1-*O*-DAG (using the cIM instrument). The 4-*O*-*α*/*β*-isomers are in dynamic equilibrium, and, as shown in the Supplementary Information (Figure S7), the peaks gave identical MS spectra.

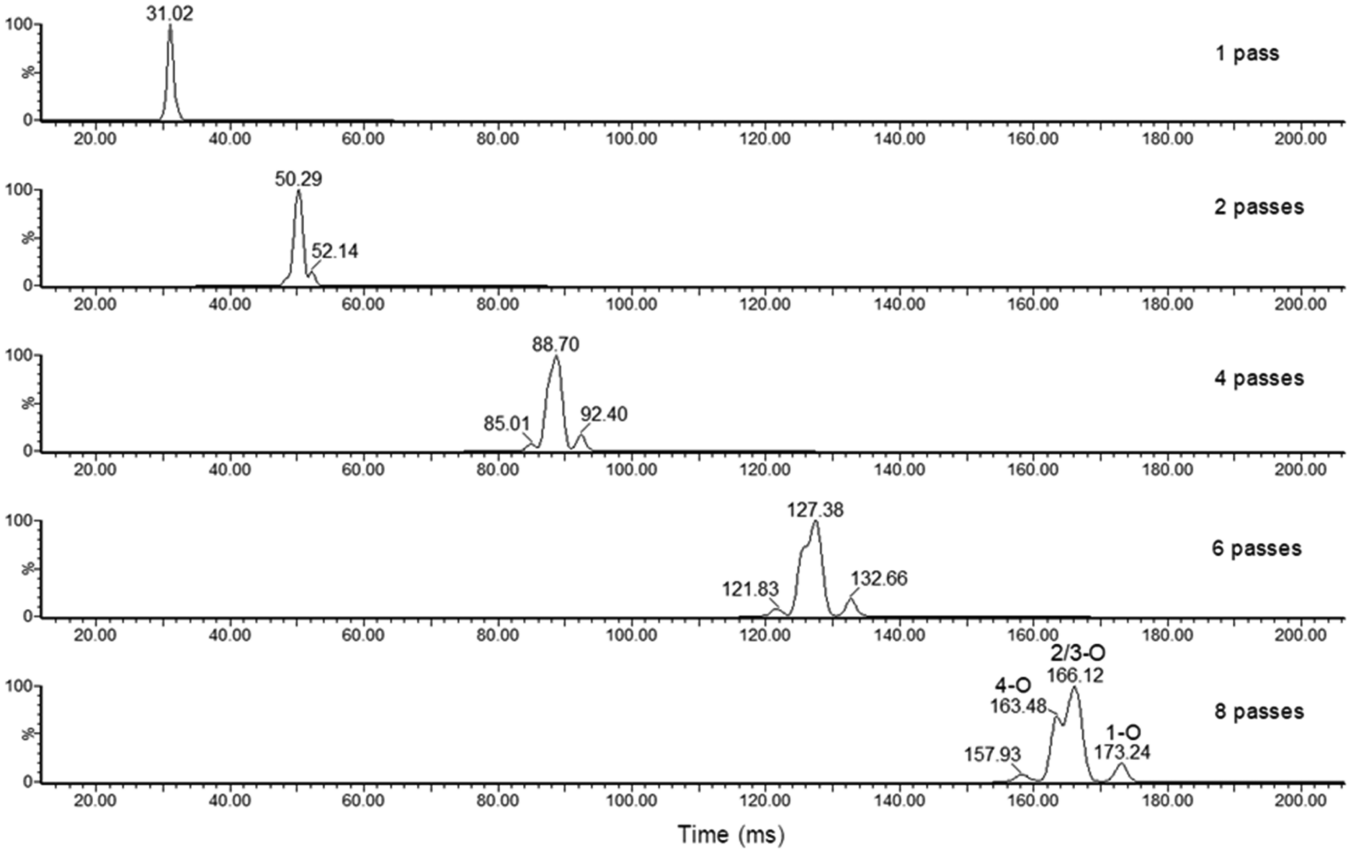

Figure 3. Comparison of the separation of DAG isomers following 1, 2, 4, 6, and 8 passes of the cIM device obtained by infusion of a sample incubated for 2 h, pH 8.5 at room temperature.

negative ion (Figure S5) modes performed on these eluting peaks confirmed that all were indeed acyl glucuronides of diclofenac. The product ion mass spectra obtained were very similar for all of the isomers. Differences were observed in the relative abundances of the fragment ions indicating differences in the relative stability of these isomers; however, no significant

https://doi.org/10.1021/acs.analchem.0c04487
Anal. Chem. 2021, 93, 7413−7421

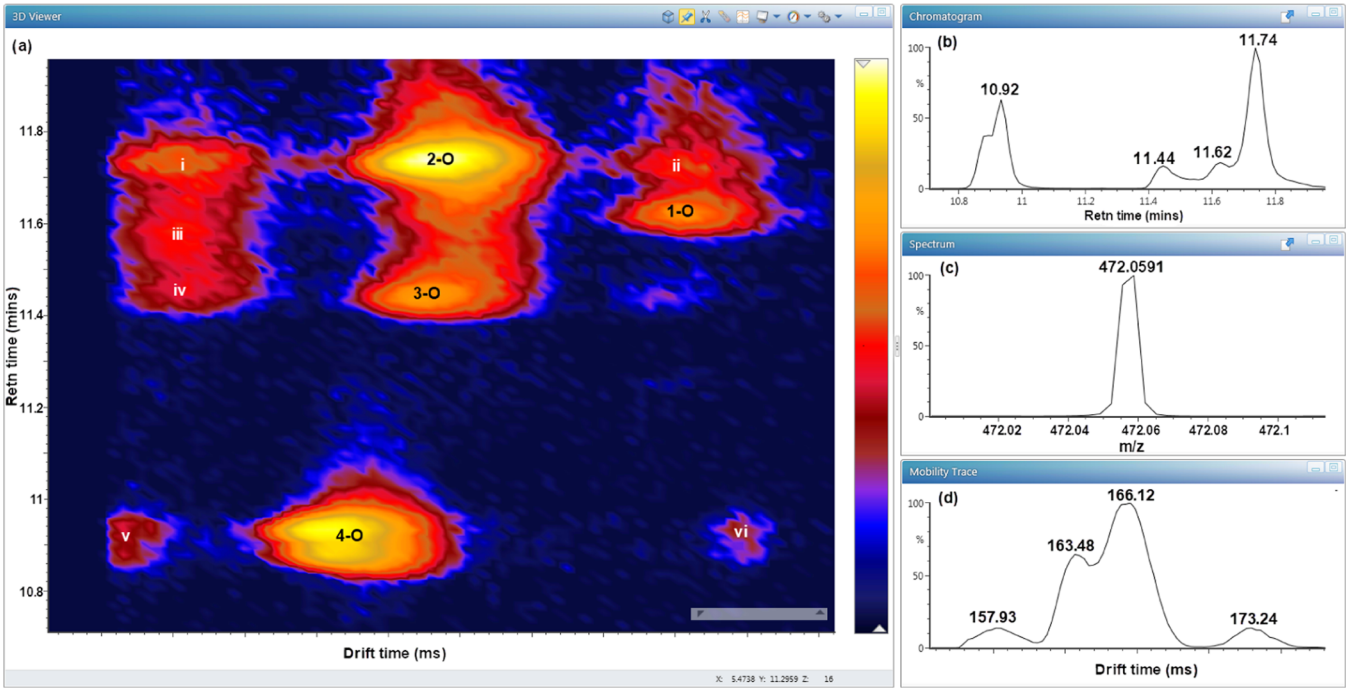

Figure 4. (a) 2D distribution of m/z 472 in the retention time range of 10.7−12.0 min following LC-cIM-MS analysis with 8 passes of the cIM device of the 120 min incubation with the regions used for selecting data in the (b) mobility filtered extracted ion chromatogram for m/z 472, (c) mass region used, and (d) ATD of m/z 472 over the time range. Peaks are identified as the 1-O, 2-O, 3-O, and 4-O isomers, while a number of partially characterized peaks i, ii, iii, iv, v, and vi are also highlighted.

differences were noted that would allow assignment of the various isomeric forms. An additional minor peak in both the MS and UV chromatograms was observed at a retention time of ∼11.23 min. The mass spectrum and product ion mass spectrum (Figure S6) of this component confirmed this peak to contain the expected chlorine isotope pattern, a dominant sodiated molecular ion, and fragment ions arising from the loss of the glucuronide moiety. It is thought that this peak may arise from the interconversion of the α/β forms of the 3-*O*-acyl species.

CCS data were also acquired after a single pass of the cyclic ion mobility device and are provided in Table 1. Comparison of $^{TW}CCS_{N2}$ values with those obtained on the linear IMS device described above showed that they were very similar in terms of their precise value and order, exhibiting less than a 0.7% difference between instruments for the four DAG species (Table 1). These data demonstrate the conservation of discrete $^{TW}CCS_{N2}$ values for the DAG species across the two platforms, which were calibrated using the same protocol, and agree with that reported previously (*e.g.*, refs 21−23). The differences in measured CCS values to the predicted values across the different isomers were 0.9−2.5% on the cIM and 0.8−2.0% on the linear device, and again the comparison of the measured $^{TW}CCS_{N2}$ with the predicted CCS values across the isomers shows that the order of CCS was consistent between measured and predicted. The relatively larger CCS predicted for the 1-*O*-isomer compared to that for the other isomers is consistent with the observed cIM separation, as is the lack of resolution of the 2/3-*O*-isomers and there was also some separation between the 2/3-*O*- and 4-*O*-isomers. We conjecture that with more examples of isomeric AGs, and perhaps more class-specific model training, it might be possible to refine the calculations as an aid to structural characterization and identification.

cIM-MS Analysis of DAG Incubations. To see if the cIM device could provide sufficient resolution for the separation of the isomeric DAGs to enable the half-life of the 1-*O*-acyl species to be measured, direct infusion of these analytes was then investigated. Initial method development was performed using a sample of the 1-β-*O*-acyl glucuronide prepared in 10 mM aqueous ammonium acetate buffer at pH 5 to ensure its stability and prevent both hydrolysis and transacylation. Unlike LC-MS, where the $[M + H]^+$ adduct was the most abundant ion, the predominant ion observed during this initial method development with infusion was m/z 510; this was assigned as the potassium adduct $[M + K]^+$ of DAG with a mass error of 0.2 ppm. Only a very weak signal was seen for the protonated molecule $[M + H]^+$, making comparison with the LC data more difficult. The solution was therefore prepared again using freshly prepared ammonium acetate in purified water from an Elga system. This provided mainly the protonated species and was used to determine initial instrumental conditions. Having established the IMS experimental parameters, further method development was performed by analysis of the sample that had been incubated in 10 mM aqueous ammonium acetate at pH 8.5 at ambient temperature for 2 h (conditions known from the LC-MS experiments to have produced a mixture of DAG isomers). The initial experiment consisted of a single pass, *i.e.*, the ions traversed the mobility device once before being ejected and subjected to mass analysis. Unsurprisingly, given the similarity of their CCS values, this experiment did not reveal any resolution of the DAG 1-, 2-, 3-, and 4-*O*-acyl isomers present in the mixture. However, as the IMS separation time was increased by a stepwise increase up to a total of 8 passes, an increase in resolution was seen. Selected arrival time distributions (ATDs) for 1, 2, 4, 6, and 8 passes are shown in Figure 3.

While, as indicated in Figure 3, no resolution was seen after a single pass, the second pass clearly revealed an additional component, with the indication of a third species. After 4 passes, all three of these components are easily observed, and, after 6

https://doi.org/10.1021/acs.analchem.0c04487
Anal. Chem. 2021, 93, 7413−7421

passes, it was clear that four components were present. Resolution was further improved after 8 passes (the maximum possible while retaining all of the components in the cIM device). This indicated that a required IMS resolution R of ~185 $\Omega/\Delta\Omega$[10] was required to resolve these components. As described above, after 8 passes, the components had filled the cIM device such that increasing the separation time further would produce "wraparound", *i.e.*, causing the first peak (highest mobility) to overtake the last peak (lowest mobility).

The LC-cIM-MS data obtained following 8 passes of the cIM device were used to compare the identification of transacylation products by LC retention time and ion mobility. The two-dimensional (2D) heat map view of ion mobility data for the LC-cIM-MS analyses is shown in Figure 4.

Comparing these data with Table 1 confirmed that the order of acyl glucuronides from low to high is 4-*O*, 3-*O*, 2-*O*, and 1-*O* with good separation of the 4-*O* and 1-*O* isomers, while the 3-*O* and 2-*O* species remained unresolved even after 16 passes (Figure S8). Additional peaks coeluting with the 2-*O*, 1-*O*, 3-*O*, and 4-*O* (peaks i and ii, iii, iv, and v and vi, respectively) components are also shown in Figure 4. These may arise from the presence of both the α/β-anomeric forms of the respective AGs as, as indicated above, these are known to interconvert on the LC time scale.[19] Alternatively, they may represent protomers of these AGs or potential boat and chair conformations of the glucuronic acid moiety. The mobility selected mass spectra for these peaks are shown in Figure S8, and these data show similar ions to those observed for the major isomers.

From these data, it was determined by comparison of the responses observed with those seen by infusion that the 1-*O*, 2/3-*O*, and 4-*O* isomers had arrival times following 8 passes of approximately 173.2, 163.5, and 166.1 ms, respectively, under the conditions employed. After ejection of the component with a drift time of 157.9 ms and the 1-O isomer (173.2 ms), the remaining components were further separated. After a further 8 passes (16 in total, ~260 $\Omega/\Delta\Omega$), increased separation of the retained components was observed and further separation of the 4-*O*-isomer from the 2/3-*O*-isomer mixture was observed although separation of the 2-*O* and 3-*O* components was not seen (Figure S9). The data from this experiment were utilized to provide a more accurate measurement of the response derived from 4-O anomers and the 2/3-O isomers.

The 1-*O*-acyl isomer was well separated from the other isomers by the cIM and, while not resolving all of the other isomers, was therefore clearly suitable for transacylation reaction monitoring and determination of the half-life of the 1-*O*-acyl form of DAG. As such, it would therefore be useful as a means of generating this surrogate measure of reactivity. To demonstrate this application, DAG was added to 10 mM ammonium acetate buffer at pH 8.5. As the purpose of this experiment was simply to demonstrate the potential for the use of the cIM system for measurement of transacylation rates, the study was performed at an ambient temperature (~20 °C), with a pH of 8.5 used to accelerate the transacylation rate. The reaction was then monitored on the instrument with data acquired from 5 min at various intervals up to 5 h. At each time point, data were acquired using 8 passes and, with isolation, 16 passes as described above. Responses were obtained by integrating the peaks in the 8-pass ATD plot data, and the area for the partially resolved peaks was proportioned using the relative response obtained from the 16-pass ATD data. The relative response of the various isomers determined by integrating the peaks in the ATDs is shown in Table 2. In Figure 5, the rapid depletion of the 1-*O*-acyl species and the sequential appearance of the other species, as would be expected, is shown obtained in this way. For comparison, the usual approach for monitoring the transacylation, *i.e.* measurement of the various isomers with a single LC-MS analysis for each time point, is shown in Figure 5a. The LC-MS data shows a similar pattern to the infusion data; however, as illustrated by the uneven degradation profiles, there was perhaps greater variability compared to the infusion study.

Table 2. Response of Various Isomers Observed in the Incubation at pH 8.5 Expressed as Percentage of the Total Response at a Given Time Point Following Analysis by Infusion into the cIM-MS

	normalized response (%)		
incubation time (h)	1-*O*-acyl	2/3-*O*-acyl	4-*O*-acyl
0.083	37	58	0
0.25	29	65	2
0.5	23	69	4
1.0	15	68	13
1.5	11	63	22
2.0	10	57	28
2.5	8	55	33
3.0	7	49	40
3.5	6	46	43
4.0	6	42	48
5.0	5	40	50

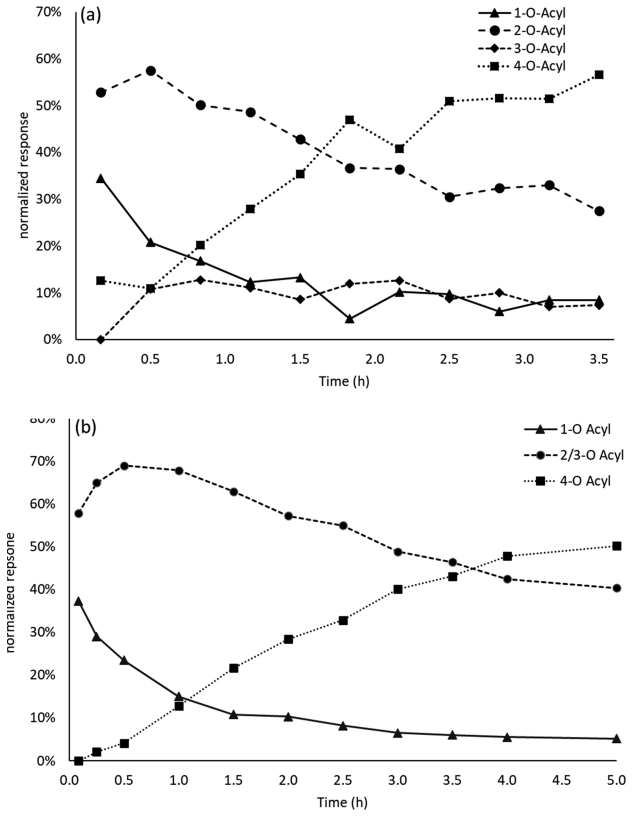

Figure 5. (a) Relative amounts of 1-*O*-, 2-*O*-, 3-*O*-, and 4-*O*-DAG observed over 0−3.5 h when incubated at pH 8.5 at room temperature, obtained by LC-MS analyses on the Synapt XS. A single measurement was made at each time point. (b) Relative amounts of 1-*O*-, 2/3-*O*-, and 4-*O*- DAG observed from 0 to 5 h when incubated at pH 8.5 at room temperature obtained by infusion and with multiple-pass analysis of the cIM device.

https://doi.org/10.1021/acs.analchem.0c04487
Anal. Chem. 2021, 93, 7413−7421

Under these experimental conditions, the initial half-life (measured up to 1.5 h) for the disappearance of the 1-*O*-DAG was 0.81 h, which is in good agreement with an LC-IM-MS value of 0.95 h and demonstrates the validity of measuring stability using infusion with cIM-MS analyses. The kinetic distribution for the disappearance of 1-*O*-DAG is shown in Figure S1. For comparison, a half-life of 0.7 h obtained in buffer at pH 7.4 and at 37 °C has previously been reported.[2]

The reactivity of acyl glucuronides has been the cause of concern, *e.g.*, refs 3−6 for many years because of their possible toxicity. As a result, there has been much research into methods for determining the stability of the 1-*O*-acyl glucuronides (and their transacylation rates), which have been used as surrogates for potential toxicity. These methods have employed a range of analytical techniques including, *e.g.*, LC-UV,[8] LC-MS,[9,20,25,26] NMR spectroscopy,[7,9,20] and LC-NMR spectroscopy.[19] The results described here show the potential of ion mobility, using the cIM device, to rapidly determine the transacylation kinetics of acyl glucuronides such as DAG. The speed with which this can be performed means that even very rapidly transacylating AGs could be measured in real time *via* constant infusion or rapid sampling techniques, and these experiments could be performed at physiological pH and temperature. Modern autosamplers have a cycle time of 1 min or lower; therefore, it would be facile to obtain 60 data points per hour, which is superior to the throughput that can be achieved by other techniques. Alternatively, the transacylation rates of a number of separate incubations (*e.g.*, of either a range of different AGs or the same AG incubated at different pH values, etc.) could be rapidly determined in the same experiment allowing the screening of the likely reactivity of such metabolites to be conducted as a routine part of drug discovery.

CONCLUSIONS

The cIM instrument was demonstrated to be able to separate the 1-*O*-acyl and 4-*O*-acyl glucuronide isomers of diclofenac, both from each other and from the 2/3-*O*-acyl isomers. The methodology was rapid compared to more conventional LC-based methods (ms vs min) and would, with development, enable near-"real-time" transacylation kinetics to be performed. While the CCS predictions that were made were not in complete agreement with the actual measured CCS values for the DAG transacylation products, they did correctly predict that separation might be possible and that the 2- and 3-*O*-acyl isomers would be the most difficult to resolve. Under the conditions employed, the 2- and 3-*O* isomers were not resolved; however, with further investigations or IMS development, the separation of even these isomers might be possible. While too much should not be read into the results for a single acyl glucuronide, should this ability to separate the 1-*O*-acyl form from the transacylated products extend to the acyl glucuronides of other compounds, this could offer considerable benefits. Thus, while both LC-MS and cIM can be used to determine transacylation kinetics, the latter is much faster and provides the potential for high-throughput analysis of these reactive metabolites.

ASSOCIATED CONTENT

Supporting Information

The Supporting Information is available free of charge at https://pubs.acs.org/doi/10.1021/acs.analchem.0c04487.

Disappearance of 1-*O*-DAG in a buffer incubated at room temperature at pH 8.5 (Figure S1); predicted CCS values from machine learning and MOBCAL vs experimentally determined values (Figure S2); arrival time distribution plots of DAG isomers formed by incubation at pH 8.5 using LC-IM-MS (Figure S3); positive ion mass spectra of 4-*O*-, 3-*O*-, 1-O-,and 2-*O*-acyl isomers following LC-cIM-MS (Figure S4); product ion mass spectra of $[M - H]^-$ (m/z 470), for 4-*O*, 3-*O*,1-*O*, and 2-*O* isomers (Figure S5); positive ion mass spectrum and product ion mass spectrum of $[M + H]^+$ (m/z 472) for thecomponent with a retention time of ∼11.23 min (Figure S6); production mass spectra of $[M + H]^+$ (m/z 472) for individual 4-*O*-α/β isomers with retention times of ∼10.84 and 10.93 min (Figure S7); positive ion mass spectra for the additional peaks (i−vi) observed in addition to major acyl glucuronide species following LC-cIM-MS analysis with 8 passes of the cIM device (Figure S8); and arrival time distribution plots for DAG isomers after 8 or 16 passes in the cIMS (Figure S9) (PDF)

AUTHOR INFORMATION

Corresponding Authors

David Higton − *Waters Corporation, Wilmslow SK9 4AX, U.K.*; orcid.org/0000-0001-7244-6536; Email: david_higton@waters.com

Ian D. Wilson − *Division of Systems Medicine, Department of Metabolism, Digestion and Reproduction, Imperial College London, London SW7 2AZ, U.K.*; orcid.org/0000-0002-8558-7394; Email: i.wilson@imperial.ac.uk

Authors

Martin E. Palmer − *Waters Corporation, Wilmslow SK9 4AX, U.K.*; orcid.org/0000-0003-1658-9334

Johannes P. C. Vissers − *Waters Corporation, Wilmslow SK9 4AX, U.K.*; orcid.org/0000-0001-6283-8456

Lauren G. Mullin − *Waters Corporation, Wilmslow SK9 4AX, U.K.*

Robert S. Plumb − *Waters Corporation, Milford, Massachusetts 01757, United States*; orcid.org/0000-0002-1380-9285

Complete contact information is available at: https://pubs.acs.org/10.1021/acs.analchem.0c04487

Author Contributions

The manuscript was written through contributions from all authors. LC-IM-MS experiments were performed by L.M. and D.H.; experimental design was by I.D.W., L.M., and D.H.; CCS computation was performed by J.P.C.V.; data interpretation and manuscript preparation were undertaken by all authors and they have given their approval to the final version of the manuscript.

Notes

The authors declare the following competing financial interest(s): D Higton, ME Palmer, JPC Vissers, LG Mullin and RS Plumb are employed by Waters Corporation.

REFERENCES

(1) Boelsterli, U. *Toxicol. Appl. Pharmacol.* **2003**, *192*, 307−322.

(2) Sawamura, R.; Okudaira, N.; Watanabe, K.; Murai, T.; Kobayashi, Y.; Tachibana, M.; Ohnuki, T.; Masuda, K.; Honma, H.; Kurihara, A.; Okazaki, O. *Drug Metab. Dispos.* **2010**, *38*, 1857−1864.

(3) Stachulski, A. V.; Harding, J. R.; Lindon, J. C.; Maggs, J. L.; Park, B. K.; Wilson, I. D. *J. Med. Chem.* **2006**, *49*, 6931−6945.

(4) Smith, D. A.; Hammond, T.; Baillie, T. A. *Drug Metab. Dispos.* **2018**, *46*, 908−912.
(5) Bradshaw, P. R.; Athersuch, T. J.; Stachulski, A. V.; Wilson, I. D. *Drug Discovery Today* **2020**, *25*, 1639−1650.
(6) FDA. Safety Testing of Drug Metabolites. https://www.fda.gov/regulatory-information/search-fda-guidance-documents/safety-testing-drug-metabolites, 2016.
(7) Farrant, R. D.; Spraul, M.; Wilson, I. D.; Nicholls, A. W.; Nicholson, J. K.; Lindon, J. C. *J. Pharm. Biomed. Anal.* **1995**, *13*, 971−977.
(8) Illing, H. P. A.; Wilson, I. D. *Biochem. Pharmacol.* **1981**, *30*, 3381−3384.
(9) Johnson, C. H.; Karlsson, E.; Sarda, S.; Iddon, L.; Iqbal, M.; Meng, X.; Harding, J. R.; Stachulski, A. V.; Nicholson, J. K.; Wilson, I. D.; Lindon, J. C. *Xenobiotica* **2010**, *40*, 9−23.
(10) Giles, K.; Ujma, J.; Wildgoose, J.; Pringle, S.; Richardson, K.; Langridge, D.; Green, M. *Anal. Chem.* **2019**, *91*, 8564−8573.
(11) Perrie, J. A.; Harding, J. R.; Holt, D. W.; Johnston, A.; Meath, P.; Stachulski, A. V. *Org. Lett.* **2005**, *7*, 2591−2594.
(12) Chen, T.; Carlos, G. In *Xgboost: A Scalable Tree Boosting System*, Proceedings of the 22nd acm sigkdd International Conference on Knowledge Discovery and Data Mining; ACM, 2016.
(13) Landrum, G. *RDKit: Open-source Cheminformatics*, 2006; p 2012.
(14) Pedregosa, F.; Varoquaux, G.; Gramfort, A.; Michel, V.; Thirion, B.; Grisel, O.; Blondel, M.; Prettenhofer, P.; Weiss, R.; Dubourg, V.; Vanderplas, J.; Passos, A.; Cournapeau, D.; Brucher, M.; Perrot, M.; Duchesnay, E. *J. Mach. Learn. Res.* **2011**, *12*, 2825−2830.
(15) Ianchis, V.; Gioioso, M.; Ballantyne, J.; Vissers, J. P. C. *ASMS Proc.* **2020**, TP 281.
(16) Broeckling, C.; Yao, L.; Isaac, G.; Gioioso, M.; Ianchis, V.; Vissers, J. P. C. *J. Am. Soc. Mass Spectrom.* **2021**, *32*, 661−669.
(17) Zhou, Z.; Tu, J.; Zhu, Z.-J. *Curr. Opin. Chem. Biol.* **2018**, *42*, 34−41.
(18) Chouinard, C. D.; Nagy, G.; Smith, R. D.; Baker, E. S. *Compr. Anal. Chem.* **2019**, *83*, 123−159.
(19) Sidelmann, U. G.; Gavaghan, C.; Carless, H. A. J.; Farrant, R. D.; Lindon, J. C.; Wilson, I. D.; Nicholson, J. K. *Anal. Chem.* **1995**, *67*, 3401−3404.
(20) Karlsson, E. S.; Johnson, C. H.; Sarda, S.; Iddon, L.; Iqbal, M.; Meng, X.; Harding, J. R.; Stachulski, A. V.; Nicholson, J. K.; Wilson, I. D.; Lindon, J. C. *Rapid Commun. Mass Spectrom.* **2010**, *24*, 3043−3051.
(21) McCullagh, M.; Pereira, C. A. M.; Yariwake, J. H. *Phytochem. Anal.* **2019**, *30*, 424−436.
(22) McCullagh, M.; Douce, D.; Van Hoeck, E.; Goscinny, S. *Anal. Chem.* **2018**, *90*, 4585−4595.
(23) Righetti, L.; Dreolin, N.; Celma, A.; McCullagh, M.; Barknowitz, G.; V. Sancho, J.; Dall'Asta, C. *J. Agric. Food Chem.* **2020**, *68*, 10937−10943.
(24) Ieritano, C.; Crouse, J.; Campbell, J. L.; Hopkins, W. S. *Analyst* **2019**, *144*, 1660−1670.
(25) Iwamura, A.; Ito, M.; Mitsui, H.; Hasegawa, J.; Keigo, K.; Kino, I.; Tsuda, M.; Nakajima, M.; Yokoi, T.; Kume, T. *Toxicol. In Vitro* **2015**, *30*, 241−249.
(26) Jinno, N.; Ohashi, S.; Tagashira, M.; Kohira, T.; Yamada, S. *Biol. Pharm. Bull.* **2013**, *36*, 1509−1513.

https://doi.org/10.1021/acs.analchem.0c04487
Anal. Chem. 2021, 93, 7413−7421